

## High Resolution X-ray Observations of Supernova Remnants

F. Bocchino \*

INAF-Osservatorio Astronomico “Giuseppe S. Vaiana”, Palermo Italy

**Abstract** The study of supernova remnants (SNRs) in the X-ray band is greatly benefiting from the availability of the large collecting area, high spatial resolution and good spectral resolution of instruments aboard XMM-Newton and Chandra satellites. The possibility of performing accurate spatially resolved spectra analysis is of course of great importance for the study of extended sources. In this review, I will briefly present a few SNR topics which, on my opinion, have greatly advanced thanks to the current generation X-ray observatories, with the aim to give a general idea on the quality of the data and the kind of research that people are doing with them.

**Key words:** supernova remnants — X-rays: supernova remnants

### 1 INTRODUCTION

It can be said that the field of supernova remnants (SNR) research is living a sort of golden era. In fact, for the first time in history, the sensitivity, spatial and, to a lesser extent, spectral resolution of the three primary bands for the investigation of SNRs, namely radio, optical and X-ray are coming closer to each other. Traditionally, the radio band has been the first option when dealing about the study of these objects, and mainstream identification criteria have been developed in this band. However, the advantage of being unaffected by interstellar absorption has been counteracted by limited sensitivity for very extended sources ( $\gtrsim 15 - 30$  arcmin) and confusion to small angular scale ( $\lesssim 5$  arcmin). The optical band offered superb spatial and spectral resolution, but high resolution studies were limited to the nearest objects for which the interstellar absorption was not an issue. On the other hand, the X-ray band used to have a clear gap with respect the radio and optical band. The sensitivity and resolution attainable were far worse than the correspondent value in other regimes, and X-rays were considered as “follow-ups” of interesting features already known in other bands. Even so, the observations made in the seventies, eighties and nineties up to the *ROSAT* satellite opened up the study of high energy processes in interstellar shocks, which are clearly of fundamental importance in the comprehension of SNRs.

With the advent of the XMM-Newton and Chandra X-ray observatories, the study of SNRs has entered for the first time the “high resolution” phase which were already common practice in radio and optical. The arcsecond spatial resolution scale obtainable with the instruments on

---

\* E-mail: [bocchino@astropa.unipa.it](mailto:bocchino@astropa.unipa.it)

board these new satellites are comparable with radio and optical observations, thus allowing for the first time detailed multi-wavelength comparison which proved to be so useful even with more modest resolution. The fine spatial resolution combined with a large collecting area is of course going to give as boost to the study of extended sources like the SNRs. Moreover, it also noteworthy that now many SNRs (or small regions of them), pulsars (PSRs) and pulsar wind nebulae (PWNe) are firstly detected in the X-ray band, thus indicating that X-ray SNR astrophysics is becoming a self-standing discipline, a thing which were not maybe obvious in the past. This, of course, does not mean that, for example, radio study should diverge from X-ray studies. On the contrary, this situation makes the need for more multi-wavelength approaches more urgent than ever, a need which the scientific community is now becoming to feel also in other topics, see for instance the forthcoming meeting “X-Ray and Radio Connections” organized by CXC, NRAO and LANL.

In this review it is my intention to show some of the SNR topics which have largely benefited from recent XMM-Newton and Chandra high resolution observations. Given the prosperity of this field and the high number of topics involved, this review will be unavoidably biased. However, I will try to cover as much aspects as possible.

## 2 ASSOCIATION BETWEEN SNRS AND COMPACT OBJECTS

Establishing connections between a SNR and the compact object which is left over the supernova explosion (if any) has always been a fascinating job, since the discovery of the Crab pulsar and its association with the nebula M1. However, the lack of compact objects and/or their direct manifestation, the pulsar wind nebulae (PWNe), inside SNRs has always been an embarrassing situation for both theoreticians and observers in this field. As Helfand & Becker (1984) had emphasized, after more than 15 year from the discovery of the Crab pulsar, there were only nine secure association between SNR and PWNe at that time, and in only three cases a pulsar was indeed detected. Since at that time the total number of galactic SNRs was around 150, the number of association seemed to be unreasonably low, even taking into account that not all the SNRs are expected to be generated by core-collapse of a massive star, and that a fraction of pulsar may be in unfavorable geometrical conditions in order to be effectively detected. For instance, it has been reported (van den Bergh & Tammann 1991) that the fraction of SNRs generated by Type II SN events (which are expected to leave a compact objects and therefore a PWN) represents  $\sim 85\%$  of the total. Moreover, Tauris & Manchester (1998) argued a beaming factor of 30%–40% for the youngest pulsars, thus combining in a fraction of 25% – 35% of detectable compact objects out of the total number of galactic SNRs.

The situation become to change with the availability of ASCA and BeppoSAX observations, which allowed for the first time a moderate spatial resolution and a large bandwidth ( $\sim 0.1 - 10$  keV), thus making the detection of non-thermal hard X-ray signals (usually from PSR and PWN) much more easy. At this stage (see Helfand 1998), it was becoming evident that the PSR-PWN manifestations were numerous but also very different from what expected on the basis of what can be extrapolated by the prototypes (mostly the Crab). Among other things, this eventually led to the introduction of the “non Crab-like” class of plerions by Woltjer et al. (1997), i.e. plerionic SNRs which have spectral properties different from the Crab Nebula and do not show the presence of a central observable pulsar, for which a non-standard evolution scenario seemed to be required.

Table 1 tries to summarize the recent advances made with (mostly but not only) XMM-Newton and Chandra observations, showing the number of known and suspect associations in 1998 (Helfand 1998) and 2002 (Kaspi & Helfand 2002), categorized both by type of SNR and by type of association (going from the most secure “Pulsar+SNR” case to the indirect evidence yielded by the presence of a “radio nebula only”). Most noteworthy is the large (65%) increase of

**Table 1** Number of Association or Suspected Association Between Compact Objects and SNRs. In Parenthesis, the Number Reported by Helfand (1998), while the Number Reported in the Review of Kaspi & Helfand (2002) is Reported Without Parenthesis. The Comparison Between the Two Numbers Allow Us to Estimate the Contribution of ASCA, BeppoSAX, XMM-Newton and Chandra to the Establishment of PSR-SNR Associations in the Last 5 Years.

Evidence	Crab-like	Composite	Shell	Total
Pulsar + SNR	(3) 3	(5) 10	(1) 2	(9) 15
Exotic/Possible NS + SNR	(1) 1	(2) 4	(9) 11	(12) 16
X-ray and radio nebula	(2) 4	(5) 5	(0) 0	(7) 9
Radio nebula only	(2) 3	(3) 5	(1) 0	(6) 8
Total	(8) 11	(15) 24	(11) 13	(34) 49
N. of known SNRs	(11) 11	(40) 42	(169) 178	(220) 231

secure associations and of association including “exotic” objects like anomalous X-ray pulsars, dim neutron stars and central compact objects, for most of which it is now possible, thanks to the new observations, to have an idea of their nature (see par. 3.3). Considering the recent advance, the expected fraction of SNR hosting a PSR-PWN, and considering that there is still evidence that we are missing 50% of the associations (Kaspi & Helfand 2002), the conclusion is that there seems to be no need anymore to invoke non-standard scenarios (i.e. creation of invisible NS) to explain the NS-SNR associations.

It would be impossible to cite all the works that has been done and that is being done on the fascinating topic about new associations between SNR and PSR-PWNe, and here I will give only a few selected reference among the most recent, thus apologizing for the many others who I omit (others can be found in Kaspi & Helfand 2002); Olbert et al. (2003) on 3C396, Claussen et al. (2002) on W28, Thorsett et al. (2002) on the enigmatic “Flying Duck”, Camilo et al. (2002a) on G54.1+0.3, Camilo et al. (2002b) on G292.0+1.8.

### 3 PULSARS AND PLERIONS

#### 3.1 Is the Crab Really the Prototype?

As I already mentioned in the previous section, the Crab nebula seems to inexorably lose its role of plerion prototype, as more and more PSR and PWNe are discovered. It seems now established that the high activity of the Crab pulsar and its nebula are the results of a particular choice of initial conditions and evolutionary scenario (not to mention the environment in which the nebula expands) which are probably not the most probable values for the plerion population. This can be more quantitatively asserted by noting the the Crab initial spin period is 19 ms while the range of the same quantity for other PWNe is 16–424ms. Moreover, the Crab nebula magnetic field is  $\sim 3 \times 10^{12}$  G, while the range for other PWNe is  $1 - 50 \times 10^{12}$  G.

The Crab is the target of a large observational project which involves Chandra and HST. The nebula was monitored with coordinated X-ray/optical observations which span almost a year and the first results were reported by Hester et al. (2002). Fig. 1 show one observation of the series. The nebula is clearly a dynamical structure, which close correlation between optical and X-ray even at small angular scales. Outward moving wisps emerging form the inner ring are clearly detected, as well as a jet. The inner ring has been temptatively interpreted as the quasi-stationary shock in the pulsar wind, but the wealth of information which can be drawn from these impressive data and the accurate comparison with the flourishing world of Crab theoretical models (e.g. Gallant & Arons (1994) a model for the wisp in Crab; Amato et al.

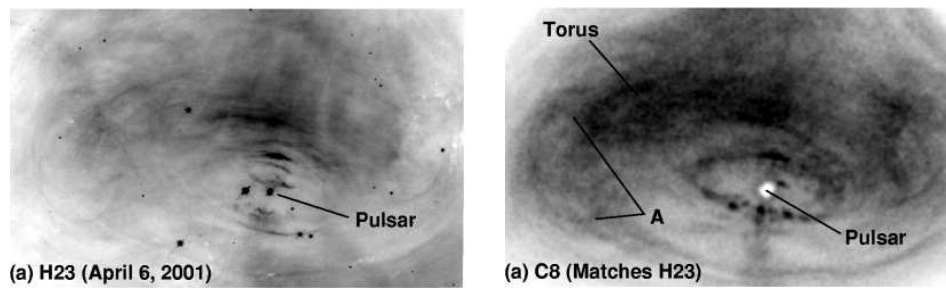


**Fig. 1** HST (*left*) and Chandra (*right*) Images of the Central Part of the Crab Nebula (Hester et al. 2002).

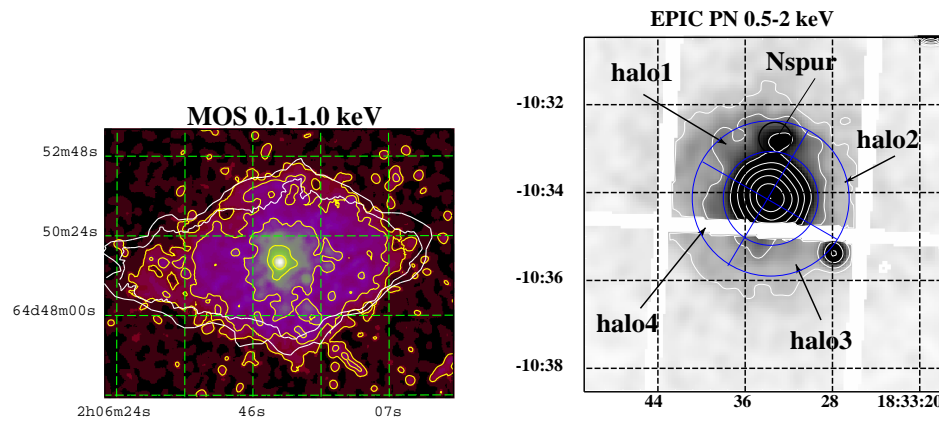


**Fig. 2** *Left*: MOS1+2 Image of 3C58 Smoothed at  $6''$ . Overlaid Are Contours Representing the Weakest ( $3\sigma = 0.15 \text{ Jy beam}^{-1}$ ) 1446 MHz Radio Contour (Bocchino et al. 2001). *Right*: EPIC PN image of G21.5-0.9 (Bocchino & Bandiera 2003).

2000 the plerions “inhomogeneous model” for their surface brightness at different wavelength; Bucciantini et al. (2003) relativistic magneto-hydrodynamical simulations of pulsar of PWNe; Arons (2002) a review of theory of pulsar winds) are still at their beginning.

### 3.2 Where Are the Shells of Pulsar Wind Nebulae?

The study of the interaction between the PWNe and their environment is potentially very interesting because it may provide constraints on the PWN evolutionary scenario. Unfortunately, the region of interaction with ISM or SNR ejecta seems to be not very active in many cases and it is often undetected. Some notable exceptions are represented by fast PSR-PWN for which a strong bow-shock is developed in the interaction region with ISM/ejecta, yielding nebulae with characteristic shapes, like in IC 443 (Bocchino & Bykov 2001).

Another interesting case is 3C58 for which a sort of confinement of radio emission is apparent (Reynolds & Aller 1988). An XMM-Newton observation has shown a remarkable coincidence between the soft X-ray emission of the nebula and its radio emission (Bocchino et al. 2001,

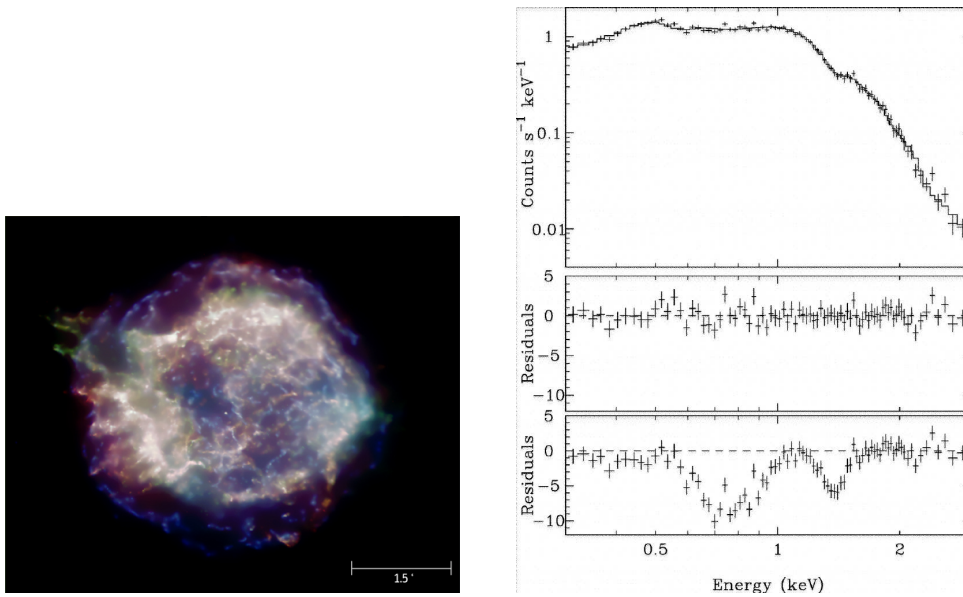


**Fig. 3** *Left:* Chandra ACIS Color Composite Image of Cas A (Hughes et al. 2000). *Right:* XMM-Newton PN spectra of compact source inside G296.5+10 (Mereghetti et al. 2002b).

Fig. 2), which is not expected since the short lifetime of electron emitting in the X-ray band. Interestingly, the outer rim of the nebula show traces of soft thermal X-ray emitting, which has been interpreted in terms of the nebula sweeping up moving ejecta, like Sankrit & Hester (1997) did for the [O III] emission detected at the edge of the Crab. This model, originally developed by Reynolds & Chevalier (1984), may explain the small amount of limb brightening and it is also in agreement with the slow shock speed measured in X-rays. It is noteworthy to mention that the long quest for the 3C58 pulsar ended last year, when it was detected for the first time by Chandra, which also revealed its high initial spin rate (Murray et al. 2002).

Yet more puzzling, the extension of the X-ray plerion G21.5-0.9 was found to be larger than the radio, as reported by Warwick et al. (2001) using an XMM-Newton observation of this object. In this case, the anomaly may be explained invoking the prominent dust scattering of X-ray photons by the interstellar dust, which seems to be consistent with the extracted X-ray profiles (Bocchino & Bandiera 2003). However, a bright spot in the halo remains unexplained (“North Spur” in Fig. 2).

### 3.3 AXPs, SGRs and other “exotic” objects

The increasing number of compact object detections in the X-ray band has revealed the large variety of manifestations of neutron stars at high energies. An emerging classification scheme include, beside the “normal” NSs which shows pulsations, the Anomalous X-ray Pulsars (slow rotators with  $P = 6 - 12$  s, strong magnetic field  $B > 10^{14}$  G, large characteristic times  $\tau_c = 10^4 - 10^5$  yr,  $L_X \sim 10^{35}$  erg s $^{-1}$ ), the Soft  $\gamma$ -ray Repeaters (SGR, which shows burst activity and a quiescent X-ray counterpart similar to AXPs) and Central Compact objects in SNRs (CCOs, with a black-body spectrum, no pulsation and  $L_X \sim 10^{33}$  erg s $^{-1}$ ).

Among the most enigmatic example in these classes there is the CCOs in Cas A, discovered in the spectacular and famous image of this object made by Chandra. The CCO has been studied by Chakrabarty et al. (2001) and also by Mereghetti et al. (2002c) with XMM-Newton, both concluding that the overall properties of this object are difficult to explain in terms of a rapidly spinning neutron star with a canonical magnetic field of  $\sim 10^{12}$  G, one of the problem being the black-body temperature too high for standard NS cooling models. There are neither radio nor optical counterparts.

One important results in NS studies came with Chandra and XMM-Newton observation of the compact object inside G296.5+10, an old thermal SNR shell. The object is a radio-quiet NS with a long period (424 ms) and a so high  $\tau_{cc} \lesssim 400$  kyr to be inconsistent with the shell age as derived in the X-ray band ( $< 20$  kyr). Sanwal et al. (2002) discovered for the first time absorption feature in its thermal spectrum and Mereghetti et al. (2002b) showed that the features are phase-dependent. Subsequently, Bignami et al. (2003), using a longer XMM-Newton observation, interpreted the observed feature as resonant cyclotron absorption, and measured for the first time the magnetic field of an isolated NS.

A good review of AXPs, SGRs and CCOs is given by Mereghetti et al. (2002a), which also summarizes possible theoretical models of this kind of objects, among which the unified scenario proposed by Alpar (2001) seems particularly appealing. According to this model, isolated NS with ordinary magnetic fields experience a mass inflow from fallback ejecta, and this causes an evolutionary phase in the propeller regime (CCOs) before the NS turns on as a radio pulsar or as an AXP. The alternative class of models invokes highly magnetized active NS (magnetars, Duncan & Thompson 1992, Thompson & Duncan 1995), but it seems that data cannot yet discriminate unambiguously between the two (Perna et al. 2001).

## 4 YOUNG SHELLS

### 4.1 Metal abundances of stellar ejecta

The young SNR shells are usually very bright X-ray objects which shows prominent line emission due to the ISM or circumstellar medium (CSM) interaction with the main or reverse shock. Abundances measures derived from fitting line fluxes and widths may be compared to nucleosynthesis models as well as model of metal mixing in the outer stellar layers. Decourchelle et al. (2001) used XMM-Newton MOS CCDs to derive maps of the Si K, Fe L and Fe K lines (Fig. 4) detecting the FeL-FeK displacement due to the reverse shock and the FeL-SiK spatial variations suggesting an incomplete mixing of the iron and silicon layers.

The dispersive X-ray spectrometers aboard Chandra and XMM-Newton offered the possibility to resolve groups of lines from single ions, thus accurately deriving the plasma ionization stage using the Lyman and helium series for light elements, or the temperature using the  $(i+f)/r$  value of helium-like triplets (O VII and Ne IX), as done for instance by Rasmussen et al. (2001). Unfortunately, spatial-spectral confusion is an important issue for extended sources observed by X-ray dispersive spectrometers, unless the SNR is very small or unless there is a bright X-ray spot in the shell.

### 4.2 Equipartition between ions and electron behind shocks

It is well known that the temperature at which particles are heated by strong SNR shocks is proportional to their mass, so electron gets a much lower temperature then ions. Eventually, ion-electron equilibration is slowly attained by Coulomb collisions in  $\sim 10^{12}/n_e$  s, but this time is longer then the typical SNR age. The topic is extremely important, since X-ray observation allows only the electron temperature to be measured, while the ion temperature does not affect

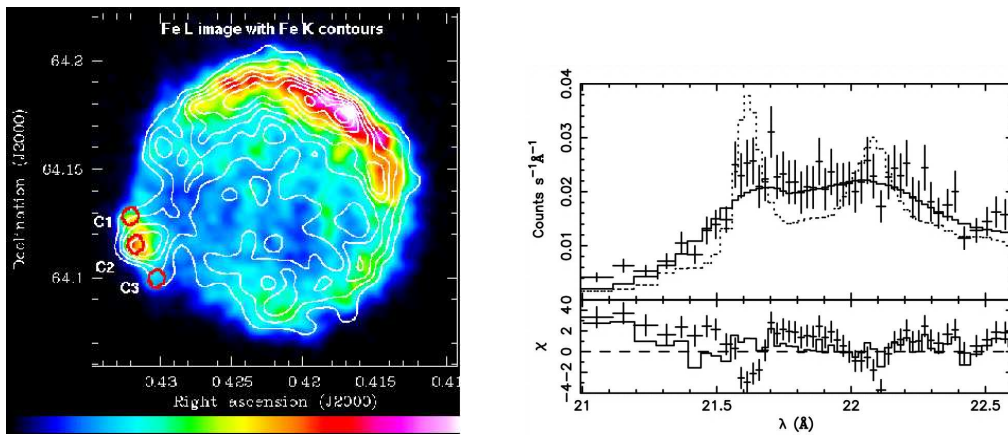


**Fig. 4** *Left:* The Tycho SNR imaged by XMM-Newton MOS in the FeL band (Decourchelle et al. 2001). *Right:* The O VII line triplet emitted by a small bright knot in SN1006 as seen by the XMM-Newton RGS (Vink et al. 2003).

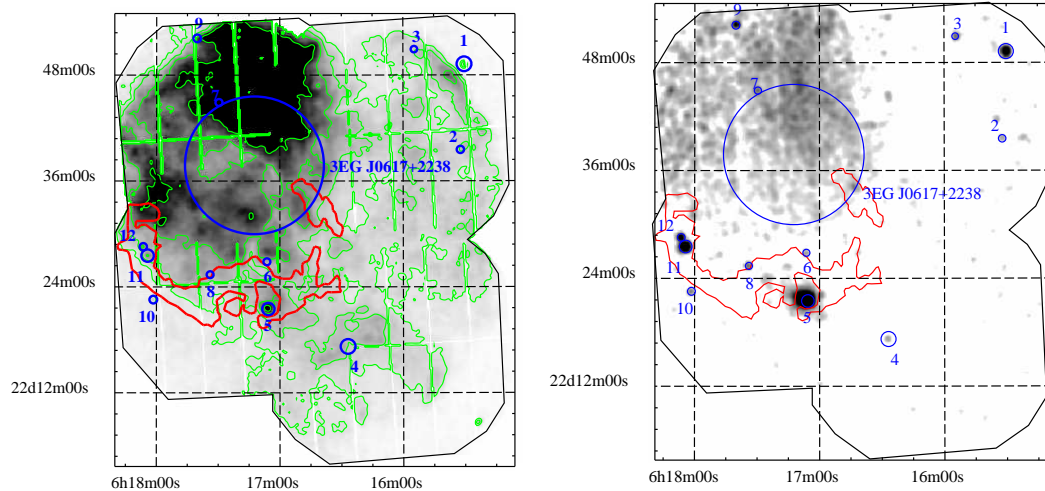


**Fig. 5** XMM-Newton PN mapping of the large SNR IC 443 at 0.5–2 keV (*left*) and at 2–10 keV (*right*, Bocchino & Bykov 2003).

the continuum and the ionization balance. Fast equilibration mechanisms have been proposed (e.g. Cargill & Papadopoulos 1988) which may lead to same electron and ion temperature at small distances behind the shock, but were traditionally difficult to verify. The CCD and grating data of a bright knot in SN 1006 obtained by XMM-Newton (Vink et al. 2003) shows that  $kT_e$  is substantially lower than the fully equilibrated value, but still higher than that expected from Coulomb equilibration alone. Doppler broadening of the O VII triplet lines measured with the RGS confirm the results (Fig. 4). Interestingly, Rakowski et al. (2003) have measured a

decreasing level of equilibration with increasing shock speed, at least in the LMC SNR DEM L71, by performing X-ray spectroscopy of the shell and fitting of the  $H\alpha$  optical line profile, which is the typical method to measure both the electron and ion temperature.

### 4.3 The Surprises of IC 443

The hard X-ray emission from the large thermal shell IC 443 has been studied in detail only recently and has shown to have a complete different morphology from the long studied soft X-ray component. Keohane et al. (1997), using the ASCA X-ray observatory, mapped for the first time the hard X-ray emission of IC 443, concluding that most of the 2–10 keV photons came from an isolated emitting feature and from the southeast elongated ridge of hard emission. BeppoSAX observations in the hard X-ray band resolved the two ASCA sources into two compact sources of hard emission up to 10 keV (1SAX J0617.1+2221 and 1SAX J0618.0+2227) and a harder component up to 100 keV, indicating that a synchrotron origin is unlikely, and suggesting electron acceleration by a slow shock in a molecular cloud (Bocchino & Bykov 2000). While recent observations of 1SAX J0617.1+2221 with Chandra (Olbert et al. 2001) and XMM-Newton (Bocchino & Bykov 2001) have established the plerionic nature of this source, the debate is still open about the nature of 1SAX J0618.0+2227. An X-ray mapping of the whole remnant by XMM-Newton has been presented by Bocchino & Bykov (2003), who show that hard emission from the field is dominated by 12 isolated source, six of which are located in a relatively small  $15' \times 15'$  region where there is strong  $2.2 \mu\text{m}$  infrared emission, indicating interaction with a molecular cloud (Fig. 5). Possible interpretations of some of the discrete sources are in terms of interaction between the SNR and the molecular cloud, possibly via bremsstrahlung of electron accelerated by slow shock in the MC (Bykov et al. 2000) or by bow shocks of fast moving ejecta in the MC (Bykov 2002).

It is important to note that IC 443 is associated with the EGRET source 3EG J0617+2238 (Esposito et al. 1996), but the relation between the remnant and the  $\gamma$ -ray source is not yet clear. In fact, the 95% error circle of the most recent-derived sky position of 3EG J0617+2238, reported by Hartman et al. (1999), does not include the plerion (see Fig. 5), and the other compact X-ray sources. Further hard X-ray studies are therefore of great importance to understand this complicated object, also in the light of the recent discovery by Uchiyama et al. (2002) of very similar features in the hard X-ray emission of the SNR  $\gamma$  Cygni observed by the ASCA X-ray satellite. Compact sources with hard emission spectra in both IC 443 and in  $\gamma$  Cygni could be of similar nature, and therefore a systematic study of SNR interacting with molecular clouds is eagerly anticipated.

## 5 MIDDLE-AGED SNR SHELLS

These kind of SNR, whose prototypes are Vela and the Cygnus Loop, are less “active” with respect to their younger fellows, since usually are undetected above  $\sim 2$  keV, most of their emission being due to the interaction between their slow main shock and the ISM (except of course the Vela pulsar region). However, these remnant are among the brightest extended soft X-ray sources in the sky, and provides valuable information on the structure, thermal characteristics and composition of the different phases of ISM, which otherwise would be very difficult to be directly derived. The gross mechanism responsible for the X-ray and optical emission of the middle-aged SNRs is well-understood: optical filaments arise from slow radiative shocks propagating in a dense and cool environment (typical density and temperature values are  $n > \sim 1 \text{ cm}^{-3}$  and  $T \lesssim 10^5 \text{ K}$ ), whereas X-ray emission originates from zones with higher temperature ( $T > 10^5 \text{ K}$ ) and lower density (usually  $< 1 \text{ cm}^{-3}$ ). However, the proper interpretation of what we see in high spatial resolution observations is still not straightforward, essentially because



the presence of clumps in the ISM disrupts the idealized spherical symmetry of the supernova explosion and its remnant, and determines local variations of the thermodynamical parameters.

For this reason, the data can be subject to several interpretations. The first scenario points out the importance of evaporation of ISM cloudlets engulfed by the main blast wave. The evaporation is caused by thermal conduction between the cooler cloud and the hotter intercloud medium (ICM) behind the shock. The second interpretation, based on cloud “bow-shocks”, invokes a complete different scenario which emphasizes the role of the overpressured regions in the post-shock flows. A third interpretation is based on the propagation of a transmitted shock inside an ISM cloud overrun by the primary blast wave. These shocks, whose presence is confirmed by numerical simulations, can be strong enough to produce X-ray emission, especially if the cloud contrast is low and/or the primary shock is fast.

### 5.1 The ISM shocked by the Vela SNR

The Vela SNR is the nearest object of its kind, located at a distance of  $\sim 250$  pc (Cha et al. 1999), and it is  $\sim 11$  kyr old. For these reasons, the Vela SNR is a privileged laboratory for the study of the interaction between the shell and the environment at a very small angular scale; each arcmin correspond to only 0.08 pc at the distance of the remnant. In particular, the North Rim of the Vela SNR has all the prototypical features of an X-ray shell expanding in a complex environment, as pointed out in several works (Bocchino et al. 1994, 1997, 1999, 2000). Two observations carried out with the ROSAT satellite in the 0.1–2.4 keV band have detected a weak background emission coming from a region not yet shocked by the blast-wave, a region with low X-ray surface brightness, and several regions with strong X-ray enhancements, both at large ( $\sim 1^\circ$ ) and small (few arcmin) spatial scales.

Bocchino et al. (2003) have reported the results of the analysis of an XMM-Newton observation of the Vela SNR North rim (Fig. 6), already studied in X-rays with ROSAT by Bocchino et al. (1999) and optically by Bocchino et al. (2000). The description of the X-ray emission of the plasma at all the investigated locations seems to require two distinct temperature components, and this seems to be different to the regions studied in Cygnus Loop by Levenson et al. (2002), Patnaude et al. (2002) and Levenson et al. (2003). Surprisingly, the value of the temperature of both components does not show significant variations in the field of view, unlike the case of Cygnus Loop. Therefore, the large variation of the surface brightness is due to variations of the relative weights of the two components, which in turns is due to difference in the line

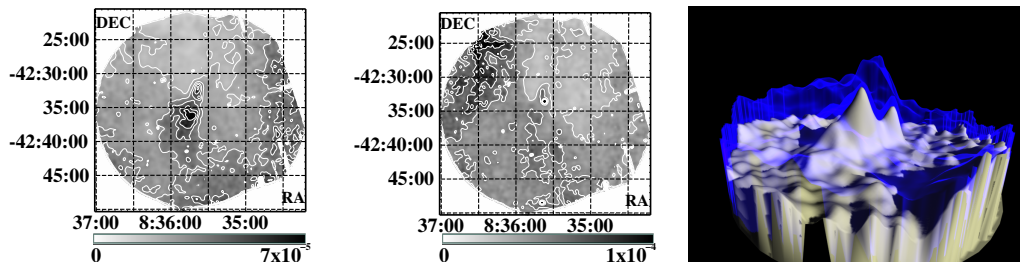


**Fig. 6** EPIC Combined Image of a Bright Knoll in the Vela SNR Shell in the 0.3 – 0.5 keV (*left*) and 0.5 – 1.0 keV Band (*center*). *Right*: 3D Model of X-ray Emitting Plasma (ISM Shocked by Main Blast Wave, Cool Component in White, Hot Component Transparent Blue, Bocchino et al. 2003).

of sight extension of the emitting plasma. An estimation of the timescales of radiative losses and thermal conduction in the detected features shows that the high temperature plasma is conduction dominated, whereas the low temperature component is radiatively dominated and both are the results of the secondary shock transmitted in a large ISM dishomogeneity.

## 6 COSMIC RAY ACCELERATION

The emerging class of non-thermal shell SNRs has been expanding in the past decade. Since these objects may play a very important role for a deeper understanding of the Galactic cosmic-ray origin, its study is of great importance. The first case was that of SN 1006, in which ASCA observations showed that the bulk of the X-ray emission has a power-law spectrum (Koyama et al. 1995 and Willingale et al. 1996). Further evidence of the presence of high-energy electrons came from the detection of TeV  $\gamma$  rays (Tanimori et al. 1998 and Aharonian et al. 2001), naturally explained in terms of inverse-Compton scattering. Recent more accurate modeling were allowed by detailed X-ray observations. Dyer et al. (2001) have derived a consistent model for spatial and spectral distribution of X-ray emission (based on emission models of Reynolds 1998), including NE-SW symmetry and deriving a current electron-acceleration efficiency of about 5%. Long et al. (2003) presented deep images of SN 1006 with the ACIS instrument on Chandra, finding no firm evidence for a halo of X-ray emission outside the shock to the northeast, as predicted by the Fermi shock-acceleration picture, and suggesting that bright rims are flattened sheets nearly perpendicular to the plane of the sky.

The shell G347.3-0.5 remarkably lacks of any signature of thermal emission, showing a featureless power continuum at any location (Slane et al. 1999), and has sometimes been referred to as the prototype of non-thermal shells. A Chandra observation reported by Uchiyama et al. (2003) has revealed a fine structure of the shell's filaments, which is typical of large SNR shells, yet confirming the extreme homogeneous character of their non-thermal X-ray emission (Fig. 7). The author conclude that this characteristic may challenge the perceptions of the standard diffusive shock-acceleration models concerning the production, propagation and radiation of relativistic particles in supernova remnants.

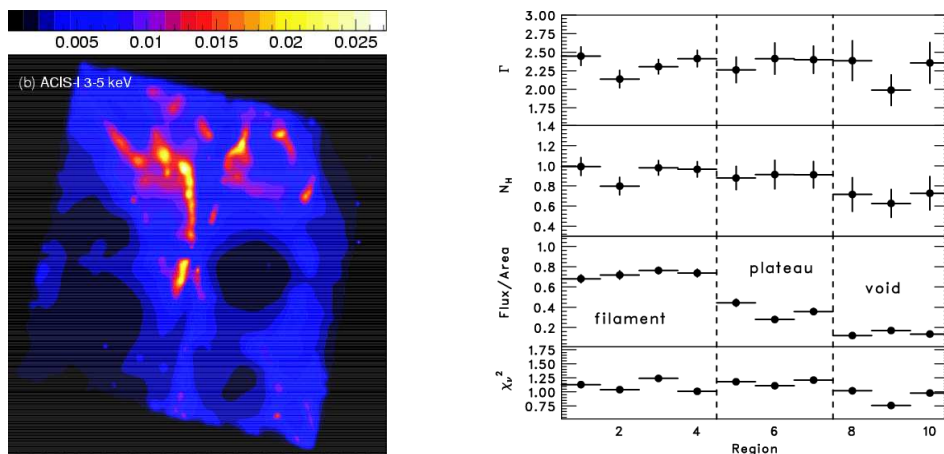


**Fig. 7** *Left:* Chandra ACIS image of a non-thermal filament in G347.3-0.5. *Right:* Result of spectral fitting of several filaments in the same SNR (Uchiyama et al. 2003).

It is still not clear if all the SNRs may explain the observed cosmic ray energy spectrum up to the observed “knee” around 1000 TeV. Reynolds & Keohane (1999) have taken a sample of SNRs with high radio surface brightness and with ASCA data available and have shown that electron acceleration seems to be active up to (at most) 80 TeV only, which seems to be confirmed by the recent studies.

So far we have reported on studies about the electron component of cosmic rays, because it is the component whose resulting emission is most easily detected. However, most of the cosmic rays are protons and there is no reason to think that the same acceleration mechanism valid for electron cannot accelerate protons as well. The signature of such a process would be the decay of pions ( $\pi_0$ ), which are generated when the protons collide with atoms and molecules in an interstellar cloud: pion decay results in  $\gamma$ -rays with a particular spectral-energy distribution. However, the predicted fluxes are not much greater than the sensitivity of current  $\gamma$ -ray detector and spectral analysis is difficult. Enomoto et al. (2002) have reported the detection of optical photons resulting from  $\gamma$ -rays at energies of  $\sim 10^{12}$  eV hitting Earth’s upper atmosphere, in the direction of the supernova remnant RX J1713.7-3946, claiming a good match to that predicted by pion decay. However, the analysis of the multi-band spectrum of this remnant made by Reimer & Pohl (2002) showed that the model adopted by Enomoto et al. (2002) is in conflict with the existing GeV data.

## 7 CONCLUSIONS

We may say that the study of SNRs is now a mature field where excellent high resolution data may be routinely compared with well-developed theoretical models, and it is not anymore only the source of nice press release images. Very low and very high densities, very strong and very weak fields, shock physics, non-linear processes are daily encountered in SNRs. However, accurate modeling requires time and in the X-ray band it has just started.

**Acknowledgements** This work was partially supported by Ministero dell’Università e della Ricerca Scientifica and by Agenzia Spaziale Italiana.

## References

- Aharonian, F., Akhperjanian, A., Barrio, J., et al. 2001, *A&A*, 370, 112  
 Alpar, M. A. 2001, *ApJ*, 554, 1245  
 Amato, E., Salvati, M., Bandiera, R., Pacini, F., & Woltjer, L. 2000, *A&A*, 359, 1107  
 Arons, J. 2002, in *ASP Conf. Ser. 271: Neutron Stars in Supernova Remnants*, 71–+  
 Bignami, G. F., Caraveo, P. A., Luca, A. D., & Mereghetti, S. 2003, *Nature*, 423, 725  
 Bocchino, F. & Bandiera, R. 2003, *Adv.Sp.Res.*, in press  
 Bocchino, F. & Bykov, A. M. 2000, *A&A*, 362, L29  
 Bocchino, F. & Bykov, A. M. 2001, *A&A*, 376, 248  
 Bocchino, F. & Bykov, A. M. 2003, *A&A*, 400, 203  
 Bocchino, F., Maggio, A., & Sciortino, S. 1994, *ApJ*, 437, 209  
 Bocchino, F., Maggio, A., & Sciortino, S. 1997, *ApJ*, 481, 872  
 Bocchino, F., Maggio, A., & Sciortino, S. 1999, *A&A*, 342, 839  
 Bocchino, F., Maggio, A., Sciortino, S., & Raymond, J. 2000, *A&A*, 359, 316  
 Bocchino, F., Miceli, M., & Maggio, A. 2003, *Adv.Sp.Res.*, in press  
 Bocchino, F., Warwick, R. S., Marty, P., et al. 2001, *A&A*, 369, 1078  
 Bucciantini, N., Blondin, J. M., Del Zanna, L., & Amato, E. 2003, *A&A*, 405, 617  
 Bykov, A. M. 2002, *A&A*, 390, 327  
 Bykov, A. M., Chevalier, R. A., Ellison, D. C., & Uvarov, Y. A. 2000, *ApJ*, 538, 203  
 Camilo, F., Lorimer, D. R., Bhat, N. D. R., et al. 2002a, *ApJ*, 574, L71  
 Camilo, F., Manchester, R. N., Gaensler, B. M., Lorimer, D. R., & Sarkissian, J. 2002b, *ApJ*, 567, L71

- Cargill, P. J. & Papadopoulos, K. 1988, *ApJ*, 329, L29
- Cha, A. N., Sembach, K. R., & Danks, A. C. 1999, *ApJ*, 515, L25
- Chakrabarty, D., Pivovarov, M. J., Hernquist, L. E., Heyl, J. S., & Narayan, R. 2001, *ApJ*, 548, 800
- Claussen, M. J., Goss, W. M., Desai, K. M., & Brogan, C. L. 2002, *ApJ*, 580, 909
- Decourchelle, A., Sauvageot, J. L., Audard, M., et al. 2001, *A&A*, 365, L218
- Duncan, R. C. & Thompson, C. 1992, *ApJ*, 392, L9
- Dyer, K. K., Reynolds, S. P., Borkowski, K. J., Allen, G. E., & Petre, R. 2001, *ApJ*, 551, 439
- Enomoto, R., Tanimori, T., Naito, T., et al. 2002, *Nature*, 416, 823
- Esposito, J. A., Hunter, S. D., Kanbach, G., & Sreekumar, P. 1996, *ApJ*, 461, 820
- Gallant, Y. A. & Arons, J. 1994, *ApJ*, 435, 230
- Hartman, R. C., Bertsch, D. L., Bloom, S. D., et al. 1999, *ApJS*, 123, 79
- Helfand, D. J. 1998, *Memorie della Societa Astronomica Italiana*, 69, 791
- Helfand, D. J. & Becker, R. H. 1984, *Nature*, 307, 215
- Hester, J. J., Mori, K., Burrows, D., et al. 2002, *ApJ*, 577, L49
- Hughes, J. P., Rakowski, C. E., Burrows, D. N., & Slane, P. O. 2000, *ApJ*, 528, L109
- Kaspi, V. M. & Helfand, D. J. 2002, in *ASP Conf. Ser. 271: Neutron Stars in Supernova Remnants*, 3
- Keohane, J. W., Petre, R., Gotthelf, E. V., Ozaki, M., & Koyama, K. 1997, *ApJ*, 484, 350
- Koyama, K., Petre, R., Gotthelf, E. V., et al. 1995, *Nature*, 378, 255
- Levenson, N. A., Graham, J. R., & Walters, J. L. 2002, *ApJ*, 576, 798
- Levenson, N. A., Graham, J. R., & Walters, J. L. 2003, in *Revista Mexicana de Astronomia y Astrofisica Conference Series*, 252–257
- Long, K. S., Reynolds, S. P., Raymond, J. C., et al. 2003, *ApJ*, 586, 1162
- Mereghetti, S., Chiarlone, L., Israel, G. L., & Stella, L. 2002a, in *Neutron Stars, Pulsars, and Supernova Remnants*, 29–+
- Mereghetti, S., De Luca, A., Caraveo, P. A., et al. 2002b, *ApJ*, 581, 1280
- Mereghetti, S., Tiengo, A., & Israel, G. L. 2002c, *ApJ*, 569, 275
- Murray, S. S., Slane, P. O., Seward, F. D., Ransom, S. M., & Gaensler, B. M. 2002, *ApJ*, 568, 226
- Olbert, C., Clearfield, R. C., Williams, N., Keohane, J., & Frail, D. A. 2001, *ApJ*, 554, L205
- Olbert, C. M., Keohane, J. W., Arnaud, K. A., et al. 2003, *ApJ*, 592, L45
- Patnaude, D. J., Fesen, R. A., Raymond, J. C., et al. 2002, *AJ*, 124, 2118
- Perna, R., Heyl, J. S., Hernquist, L. E., Juett, A. M., & Chakrabarty, D. 2001, *ApJ*, 557, 18
- Rakowski, C. E., Ghavamian, P., & Hughes, J. P. 2003, *ApJ*, 590, 846
- Rasmussen, A. P., Behar, E., Kahn, S. M., den Herder, J. W., & van der Heyden, K. 2001, *A&A*, 365, L231
- Reimer, O. & Pohl, M. 2002, *A&A*, 390, L43
- Reynolds, S. P. 1998, *ApJ*, 493, 375
- Reynolds, S. P. & Aller, H. D. 1988, *ApJ*, 327, 845
- Reynolds, S. P. & Chevalier, R. A. 1984, *ApJ*, 278, 630
- Reynolds, S. P. & Keohane, J. W. 1999, *ApJ*, 525, 368
- Sankrit, R. & Hester, J. J. 1997, *ApJ*, 491, 796
- Sanwal, D., Pavlov, G. G., Zavlin, V. E., & Teter, M. A. 2002, *ApJ*, 574, L61
- Slane, P., Gaensler, B. M., Dame, T. M., et al. 1999, *ApJ*, 525, 357
- Tanimori, T., Hayami, Y., Kamei, S., et al. 1998, *ApJ*, 497, L25+
- Tauris, T. M. & Manchester, R. N. 1998, *MNRAS*, 298, 625
- Thompson, C. & Duncan, R. C. 1995, *MNRAS*, 275, 255
- Thorsett, S. E., Brisken, W. F., & Goss, W. M. 2002, *ApJ*, 573, L111
- Uchiyama, Y., Aharonian, F. A., & Takahashi, T. 2003, *A&A*, 400, 567
- Uchiyama, Y., Takahashi, T., Aharonian, F. A., & Mattox, J. R. 2002, *ApJ*, 571, 866
- van den Bergh, S. & Tammann, G. A. 1991, *ARA&A*, 29, 363
- Vink, J., Laming, J. M., Gu, M. F., Rasmussen, A., & Kaastra, J. S. 2003, *ApJ*, 587, L31
- Warwick, R. S., Bernard, J., Bocchino, F., & et al. 2001, *A&A*, 365, L248
- Willingale, R., West, R. G., Pye, J. P., & Stewart, G. C. 1996, *MNRAS*, 278, 749
- Woltjer, L., Salvati, M., Pacini, F., & Bandiera, R. 1997, *A&A*, 325, 295